



Comparative Analysis of Fatigue Performance in Asphalt Concrete Modified with Nano-Alumina and Nano-Silica

Amjad H. Al Bayati¹ , Ali M. Al Hamdou¹ , Yu Wang²

¹ Department of Civil Engineering, College of Engineering, University of Baghdad, Baghdad, Iraq.

² School of Science, Engineering & Environment, University of Salford, Manchester M5 4WT, UK

Article Info	ABSTRACT
<p>Received: 04 Dec. 2025 Revised: 24 Dec 2025 Accepted: 12 March 2026 Available online: 31 March 2026</p> <p>Keywords: Nano-Aluminum Oxide; Nano-Silica Oxide; Asphalt binders; Fatigue Performance; Rheology; IDEAL-CT; LAS.</p>	<p>This comparative study systematically evaluated the fatigue and cracking performance of asphalt binder and asphalt concrete mixtures, modified with different dosages (2%, 4%, and 6% by binder weight) of Nano-Alumina (NA) and Nano-Silica (NS). The experimental methodology involved binder testing, including the evaluation of physical properties, rheological behaviour, and fatigue characteristics using the Superpave parameter ($G^* \sin \delta$) and Linear Amplitude Sweep (LAS) test. Additionally, compatibility was assessed through storage stability testing and Scanning Electron Microscopy (SEM). Mixture performance was evaluated using Indirect Tensile Cracking Test (IDEAL-CT) to determine the Cracking Tolerance Index (CT-Index), Flexibility Index (FI), and Crack Resistance Index (CRI). The results showed that nanomaterials substantially improved binder stiffness and thermal stability, with (NA) consistently causing the strongest stiffening effect, indicating that NA provided a stable and gradual improvement in fatigue life from 2% to 6%. (NS) showed a strong effect on increasing viscosity, achieving better initial cracking tolerance and fatigue life at low concentrations (2% to 4%). Notably, the study identified a narrow optimal range for NS; at 6%. NA provided a balanced improvement, maximizing CT-Index at 6% and CRI at 4%, while NS achieved very high CT-Index at 2% but decreased at higher dosages. Collectively, an optimal practical dosage of 2–4% for NS and 4–6% for NA are recommended, highlighting the importance of material-specific optimization to achieve better durability and fatigue life under repeated loading.</p>

1. Introduction

Fatigue cracking, one of the principal distresses affecting flexible pavements, where, repeated traffic loading is identified as the primary cause of fatigue damage and subsequent loss of serviceability [1]. Fatigue distress in asphalt cement (AC) generally occurs through two mechanisms, cohesive failure within the mastic phase and adhesive failure at the AC–aggregate interface [2]. The mechanical response of asphalt binder is governed by loading duration,

temperature, and the level of applied stress or strain. At short loading times, the binder exhibits largely elastic behavior, comparable to its response at low temperatures, due to limited time for molecular rearrangement. In contrast, elevated temperatures or prolonged loading periods (or low loading rates) promote a more viscous response [3,4].

Fatigue life varies according to mixture properties, asphalt layer thickness, loading mode and frequency, rest periods between loads, and the environmental conditions [5]. Laboratory methods

used to quantify fatigue performance may include four-point bending beam fatigue test and the indirect tensile fatigue test, conducted under either stress- or strain-controlled mode [6,7]. Numerous studies have confirmed a strong correlation between binder-level and mixture-level performance [8–10]. Additionally, extensive research demonstrated that nanomaterial modification of asphalt binders significantly enhanced pavement performance [11].

Saltan et al. [12] reported that 0.3% NS dosage produced the most favorable fatigue performance in Dynamic Shear Rheometer (DSR) testing, whereas lower or higher dosages resulted in diminished benefits. Similarly, Leiva-Villacorta et al. [13] concluded that adding (3–6% NS) improved fatigue resistance, while 0.5% produced adverse effects, highlighting the sensitivity of binder behavior to NS content. Nazari et al. [14] confirmed that (2–4% NS) extended fatigue life at all shear strain levels due to the formation of a reinforcing nano-network within the binder. Complementary results were reported by Shafabakhsh et al. [15], who found that (4–6% NS) enhanced fatigue life in both LAS and four-point bending tests, with performance declined at 8% under aging conditions. The findings designate that fatigue performance of NS-modified asphalt is highly dosage-dependent, with optimal contents varying according to binder characteristics, nano-silica properties, and the applied testing methodology.

As for NA, Eghlim et al. [16] demonstrated substantial improvements in fatigue life across a wide temperature and stress range (2–8% NA), with 8% providing the best performance due to enhanced cohesion and adhesion at the binder–aggregate interface. Karahancer et al. [17] also observed consistent gains in fatigue performance for mixtures modified with 3–7% NA, with an optimum at 5%. Bhat et al. [18] showed that low NA dosages (0.5–2%) improved fatigue response at 25°C using Time Sweep Test, while Mamuye et al. [19] reported increased CT Index values in IDEAL-CT testing for binders modified with 1–3% NA, with the highest enhancement at 3%.

The present study aims to systematically evaluate and compare the fatigue performance of asphalt binders and mixtures modified with nano-silica (NS) and nano-alumina (NA). By investigating the influence of these nanomaterials

on binder rheology and mixture cracking resistance, the research seeks to identify the optimal additive type and dosage for enhancing durability and fatigue life under static loading. Experimental procedure employed in this study is summarized in the workflow presented in Figure 1.

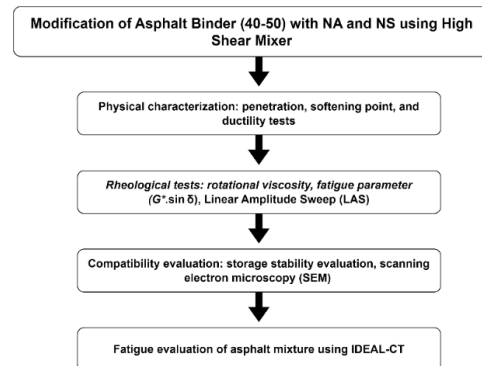


Figure 1. Workflow for Experimental Evaluation of Nano-Modified Asphalt Binders and Mixtures.

2. Materials

2.1. Asphalt Binder

Asphalt binder with penetration grade 40–50 is implemented within the course of experimental course for this study, its obtained from the Dora refinery, south-west of Baghdad. The physical and rheological properties as per the standard tests and the Superpave PG system (AASHTO M320 [20]) are summarized in Table 1.

Table 1. Physical and Rheological Behavior of 40–50 Asphalt Binder.

Property	Standard	Measured value	Limit
Penetration (0.1 mm)	AASHTO T 49	44	(40–50)
Ductility (cm)	AASHTO T 51	+100	>100
Softening point (°C)	AASHTO T 53	48.7	-
Rotational Viscosity (mPa·s)	AASHTO M 320	745	3000 (max)
G* sin δ (kPa) (70 °C and 76 °C)	AASHTO M 320	1.45 and 0.70	1.00 kPa (min)
Mass loss (%)	AASHTO M 320	0.254	1% (max)
G* sin δ (kPa) (22°C and 25 °C)	AASHTO M 320	6796 and 5019	5000 kPa (max)

2.2. Nanomaterials

Two inorganic nanomaterials are implanted in this study, these are NS and NA. They were added to asphalt binders to improve performance. NS increases viscosity, stiffness, and fatigue resistance due its fine, porous structure as well as high surface area [24], in the other hand, NA enhances stiffness, thermal stability, and crack resistance via mechanical interlocking [25]. The physical properties of NS and NA employed in this study are summarized in Table 2. Scanning Electron Microscopy (SEM) analysis (Figure 2) revealed the distinct microstructural features of NS and NA, providing a microstructural basis for the observed improvements in rheological and mechanical behavior of the modified asphalt binders. In this study, both NS and NA were incorporated at dosages ranging from 2% to 6% by binder weight, which were selected to optimize the balance between enhanced stiffness and fatigue performance while maintaining acceptable workability and minimizing the risk of particle agglomeration.

Table 2. Physical Characteristics of Nano-Silica and Nano-Alumina.

Properties	Nano-Alumina	Nano-Silica
Chemical formula	Al ₂ O ₃	SiO ₂
Appearance	White Powder	White Powder
Average particle size (nm)	10–20	25–35
Purity (%)	99.9	99.8
Specific surface area (m ² /gm)	120–160	190–250
Bulk Density (g/mL)	0.2	0.08
Nanomaterials Prices (USD/kg)	28.5	26.8

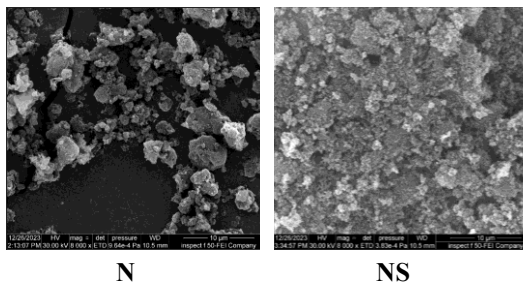


Figure 2. SEM images of nanomaterials used in asphalt modification at 8,000× magnification.

2.3 Aggregate Materials

The study used Type D5 aggregate gradation per ASTM D3515 [26], ensuring dense-graded mixtures with adequate durability, stability, and resistance to traffic deformation. The gradation and limits are shown in Figure 3

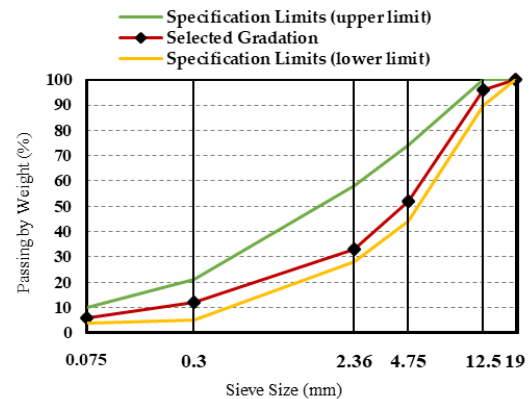


Figure 3. Gradation and Specification Limits of Surface Coarse Aggregates.

3. Preparation of Test Specimens

The selection of mixing and blending procedures for nano-modified asphalt binders therefore often depends on expert judgment. Following this approach, Al-Bayati et al. [27] incorporated nano-silica, titanium, and alumina at dosages of 2%–8% by binder weight, employing a dry mixing process at (140 °C, 4000 rpm, 20 minutes), with nanomaterials added at a rate of 4 g/min. In the present study, NS and NA were added at 2%–6% by binder weight to 500 g of asphalt. Initial blending was conducted using a high-shear mixer at 400 rpm, with 10 g of nanomaterials introduced gradually over 4 minutes (2.5 g/min) at 140 °C, then subjected to high-shear mixing (3000 rpm) at 140–150 °C for 20 minutes to ensure uniform dispersion.

4. Experimental Methodology for Materials Testing

4.1 Evaluation of Physical Properties

In the scope of this research, a series of standardized tests were performed on asphalt binders to determine their performance characteristics. To evaluate the consistency of the binder, the Penetration Test was conducted in accordance with ASTM D5-06. The binder's thermal susceptibility, an indicator of its

performance at high in-service temperatures, was assessed using the Softening Point Test as specified by ASTM D36-06. The binder tensile deformation capacity for was evaluated using ductility tests at 25 °C as per the ASTM D113. Collectively, these tests provide a comprehensive characterization of modified binder fundamental behavior.

4.2 Evaluation of Rheological Properties

4.2.1 Rotational viscosity (RV)

This parameter was measured to evaluate flow behavior at elevated temperatures, which is critical for mixing and compaction processes. Testing was conducted according to AASHTO T316, using a rotational viscometer at 135 °C.

4.2.2 Fatigue parameter assessment of asphalt binders

For the Pressure Aging Vessel (PAV) aged which simulated asphalt binder field condition (after placement), fatigue parameter $G^* \sin \delta$ was assessed using the Anton Paar – Smart Pave 102e Dynamic Shear Rheometer (DSR) system (figure 4), following the procedures outlined in AASHTO T315. [28]. The assessment aimed to characterize the viscoelastic response under repeated loading and resistance to fatigue cracking. The fatigue parameter ($G^* \sin \delta$) was measured at 25 °C, specification limit of 5000 kPa was applied to control fatigue susceptibility.

4.2.3 LAS test

Linear Amplitude Sweep (LAS) test on a DSR with 8 mm parallel plates and a 2 mm gap (figure 5) was conducted following AASHTO T391 and T315. Binder samples were aged via RTFOT (AASHTO T240) and PAV (AASHTO R28) prior to testing. The test included a frequency sweep at 0.1% strain 0.2–30 Hz (linear viscoelastic behavior), followed by an amplitude sweep at 10 Hz with strain increasing from 0% to 30% over 3100 cycles. Shear strain, shear stress, phase angle (δ), and complex modulus (G^*) were recorded, and fatigue life (Nf) was predicted using the VECD framework (Equation 1).

$$Nf = A(Y_{max})^{-B} \quad \text{Eq. (1)}$$

Where: Y_{max} = estimated maximum strain anticipated within the pavement structure, A = describes the binder's damage evolution behavior

and B = intrinsic property of the binder in its undamaged state.



Figure 4. Smart Pave

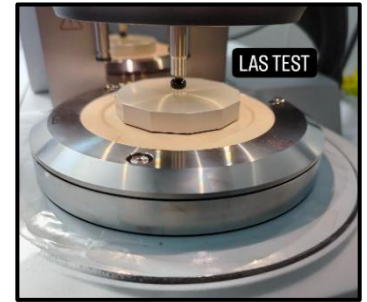


Figure 5. LAS test.

4.3 Compatibility Assessment

The asphalt binders' storage stability was assessed by placing the materials in aluminum tubes (14 cm × 3.5 cm), sealing them, and storing them vertically by conditioning at 163°C for 48 hours. After cooling, each tube was sectioned into three equal parts, and the softening points of the top and bottom segments were determined. A temperature stability difference of 2.5 °C or less was regarded as acceptable, whereas larger differences signaled phase separation [32,64].

Microstructural characterization was performed using a VEGA- II apparatus (up to 2000×) to examine particle distribution and dispersion within the binder.

4.4 Marshall Mix Design

The test was performed according to ASTM D6926 [33]. Specimens were compacted with 75 blows per face. Stability, flow, air voids, and VMA were determined following ASTM D6927, D2726, and D2041 [34–36]. The control mixture's optimum asphalt content was established at 5.0% and consistently applied to all nano-modified mixtures, ensuring that performance differences were exclusively due to the type and concentration of nanomaterials.

4.5 Evaluation of Asphalt Mixture Fatigue Performance

The Indirect Tensile Cracking Test (IDEAL-CT) was conducted to evaluate the fatigue resistance of asphalt concrete specimens with dimensions of 101.6 mm (4 in.) in height and 63 mm (2.5 in.). This test, known for its simplicity

and efficiency, involved subjecting the cylindrical specimens to a consistent vertical load, recording load and displacement data. The specimens were compacted to an air void level of around ($4 \pm 0.5\%$) using a Marshall compactor. The test was conducted following ASTM D8225 [37], During the test, specimens were loaded diametrically at 50 mm/min and tested at 25 °C using a 12.7 mm loading strip. Each set of samples was tested in triplicate, and the average results were reported. CT Index was calculated using Equation (2).

$$CT_{Index} = \frac{t}{62} \times \frac{i_{75}}{D} \times \frac{G_f}{m_{75}} \times 10^6 \quad \text{Eq. (2)}$$

Where: G_f = fracture energy, m_{75} = post-peak slope at 75% of the peak load, i_{75} = displacement at 75% of peak load during IDEAL-CT test.

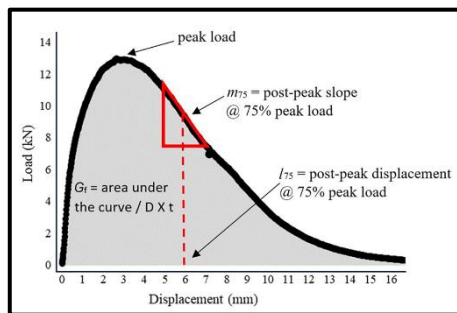


Figure 6. IDEAL-CT load-displacement curve.

The Flexibility Index (FI) and Crack Resistance Index (CRI) were calculated to provide a more comprehensive analysis of the fatigue behavior of the asphalt mixtures [38]. The FI was determined using Equation (3), while the CRI was evaluated using Equation (4):

$$FI = \frac{G_F}{|m|} \times 0.01 \quad \text{Eq. (3)}$$

Where: FI = flexibility index, G_f = fracture energy (J/m²), m = post-peak slope (kN/mm),

$$CRI = \frac{G_F}{P_{max}} \quad \text{Eq. (4)}$$

Where: CRI = Crack Resistance Index, G_f = fracture energy and p_{max} = peak load.

5. Results and Discussion

5.1 physical test Results

The physical properties (figure 7-9) demonstrate that incorporating NA and NS

noticeably enhanced binder consistency and thermal stability relative to the neat asphalt. Penetration decreased substantially with nano-aluminum, falling from 44 to 22 (0.1 mm), representing a 50% reduction, while nano-silica produced decreases of 4.5%, 2.3%, and 13.6% at 2%, 4%, and 6%, respectively confirming increased hardness for both modifiers. Softening point improved consistently, with nano-aluminum increasing it by 11.3%, 11.0%, and 14.6%, and nano-silica producing increases of 10.1%, 8.0%, and 17.5%, reflecting enhanced high-temperature stiffness. Ductility remained unchanged at 100 cm for all nano-aluminum dosages and for nano-silica up to 4%, while a slight decline to 95 cm (5% decrease) at 6% nano-silica suggests a minor reduction in elongation only at higher loading. The improvement in softening point with nano-aluminum is attributed to the formation of a nanoparticle network that enhances thermal stability [39], consistent with previous findings [40,41]. For nano-silica, the increases in hardness and softening point are related to its adsorption of light volatiles, rise in asphaltene content, and strong molecular interactions resulting from its high surface area and reactive surface chemistry, which enhance interaction with the asphalt matrix [42,43], consistent with findings from previous studies that reported similar improvements in binder stiffness upon nanomaterial incorporation [44,12,45].

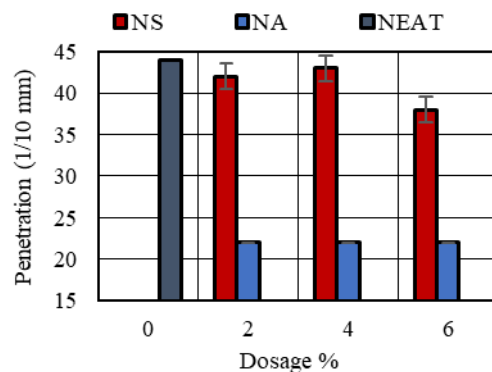


Figure 7. Penetration of nano-modified asphalt.

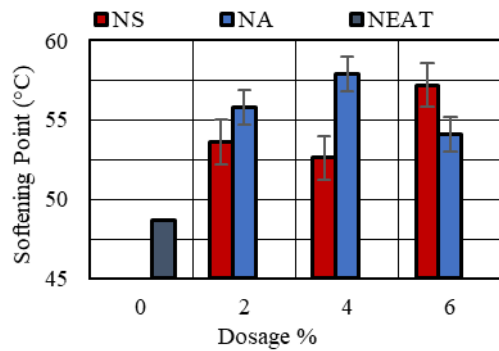


Figure 8. Softening of nano-modified asphalt.

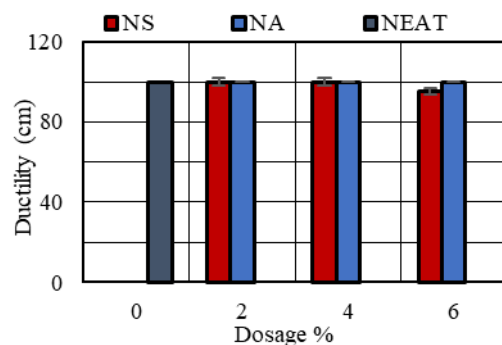


Figure 9. Ductility of nano-modified asphalt.

5.2 Evaluation of Rheological Properties

5.2.1 Rotational Viscosity Assessment

The results of RV exhibited in Figure 10 show a clear stiffening effect resulted from the use of both nanomaterials, i.e. nano-aluminum oxide (Al_2O_3) and nano-silica (SiO_2), as all modified binders showed higher viscosity than the neat asphalt (745 mPa·s). For nano-aluminum, RV increased to 1112, 1214, and 1245 mPa·s at 2%, 4%, and 6%, corresponding to 49.2%, 62.9%, and 67.2% increases. NS displayed a similar pattern, with RV rising to 1129, 1183, and 1368 mPa·s, representing increases of 51.5%, 58.8%, and 83.6% of each dosage respectively. Strong viscosity-building effect of nano-silica is attributed to high surface area and reactivity [46], absorption of maltene components which increases asphaltene content [47], and the diffusion of silica particles into the binder that reduces oily fractions and introduces stiffer solid phases [48]. Additionally, the hardening effect is reinforced by improved dispersion of NS layers, which could result in an improved bonding strength via restricting binder flow [49]. For NA, the viscosity increase arises from its stiffening effect and high surface area that increases particle

interactions and promotes stronger attraction with surrounding asphalt molecules [19], further supported by better dispersion that limits binder mobility and strengthens the matrix [50].

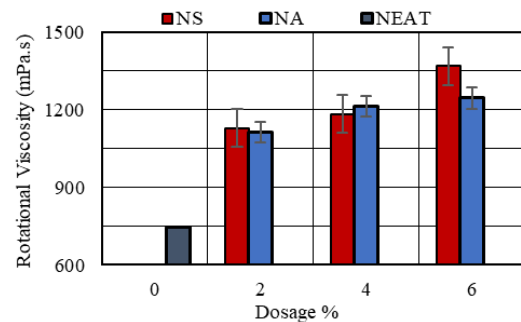


Figure 10. Viscosity Behavior of Modified Asphalt Binder

5.2.2 Results of the Rheological Fatigue Indicator ($G^* \cdot \sin \delta$)

The $G^* \cdot \sin \delta$ fatigue parameter in Figure 11 reflects the influence of nano-aluminum oxide (Al_2O_3) and nano-silica (SiO_2) on the binder's susceptibility to fatigue cracking. For NA, the 2% dosage produced a slight increase (1.0%), indicating no improvement in fatigue performance, whereas the 4% and 6% dosages resulted in substantial reductions of 28.2% and 15.2%, respectively. A notable enhancement in the binder's fatigue resistance at intermediate and higher contents, is likely due to improved viscoelastic balance and greater energy dissipation capacity under repeated loading. NS at 2% and 4% produced identical reductions (15.4%). The 6% NS produced an increase of 11.4, possibly due to particle agglomeration or excessive stiffening that limits the binder's ability to dissipate strain energy. Both nanomaterials enhanced fatigue performance at specific optimal dosages, confirming their ability to improve the resistance to microcrack initiation and propagation, findings are consistent with the previous studies reporting fatigue resistance improvements in nano-modified asphalt binders [50, 51, 52].

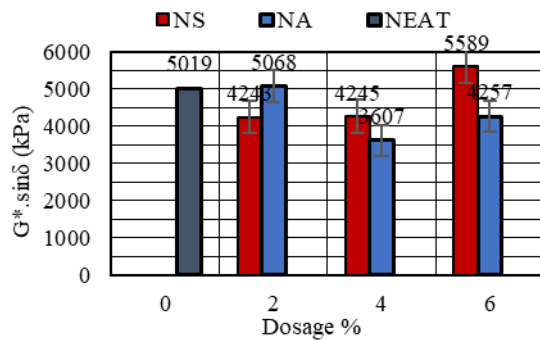


Figure 11. $G^* \cdot \sin \delta$ for Neat and Nano-Modified Asphalt Binders (25 °C).

5.2.3 LAS Test Results

The incorporation of nanoparticles altered the mechanical behavior and fatigue performance of asphalt binders, with distinct effects observed for NS and NA. When comparing the NEAT binder which exhibited the highest ultimate shear stress, modified binder with 2%, 4%, and 6% NS showed slightly reduced peak stresses, with corresponding strains at maximum stress of 19.1%, 20.1%, and 18.1%, respectively. The reduction in ductility at higher NS dosages, particularly at 6%, suggests that excessive nanoparticle addition slightly stiffen the binder matrix, restricting large deformations prior to failure. Despite this modest reduction in peak stress, fatigue life was substantially enhanced across both 2.5% and 5% strain levels, with the greatest improvement observed at 2% NS (16.6×10^6 and 6.42×10^5 cycles), followed by minor decreases at 4% (16.17×10^6 and 6.31×10^5 cycles) and 6% (16.08×10^6 and 5.46×10^5 cycles). This pattern emphasized the existence of an optimal NS dosage, beyond which benefits plateau or slightly diminishes. The improvements are mostly attributed to high specific surface area, which promotes uniform dispersion, strengthens the internal microstructure, and delays microcrack initiation [53, 54, 55].

For NA, the strain at ultimate stress decreased with increased dosage, from 20.11% for the NEAT binder to 19.10%, 18.09%, and 17.13% for 2%, 4%, and 6% NA, respectively. Unlike NS, the fatigue performance of NA-modified binders exhibited a consistent, dose-dependent improvement across both strain levels, with fatigue life increasing from 9.64×10^6 and 3.84×10^5 cycles for the NEAT binder to 1.59×10^7 , 1.81×10^7 , and 2.08×10^7 cycles at 2.5% strain, and 5.80×10^5 , 7.04×10^5 , and 8.35×10^5 cycles at 5% strain for 2%,

4%, and 6% NA, respectively. NA ability to reinforce the binder matrix, improve microstructural integrity, enhance energy dissipation, and delay crack nucleation and propagation under repeated loading led to its superior performance [56, 57]. While both NS and NA improved fatigue resistance, NS showed better performance at lower dosages due to potential agglomeration at higher contents, whereas NA provided consistent, dose-dependent reinforcement, this emphasized the importance of nanoparticle type and dosage optimization. Figure 12 depicts the stress–strain behavior of asphalt binders modified with different nanoparticles, whereas Figure 13 shows the corresponding fatigue life curves.

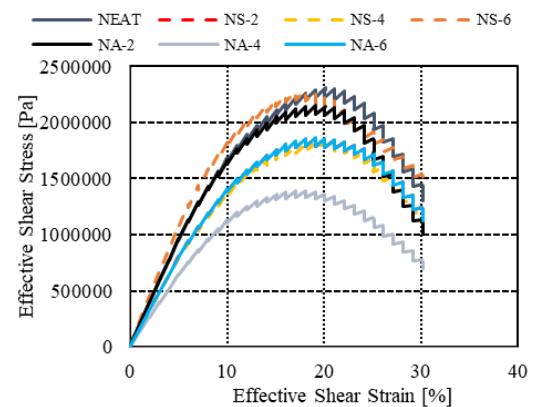


Figure 12. Characterization of Shear Stress–Strain Performance in Nanommodified Asphalt Binders

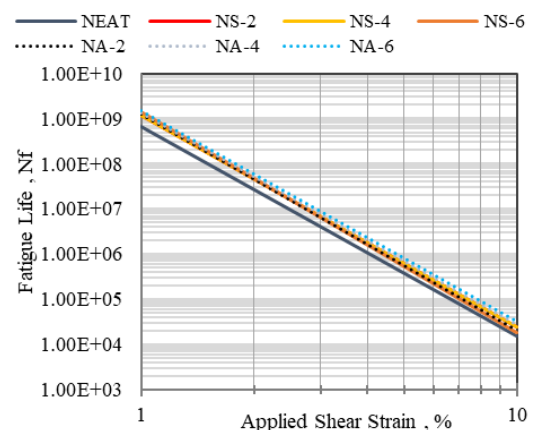


Figure 13 Fatigue Life Response of Asphalt Binders Modified with Nanomaterials

5.3 Results of the Compatibility Assessment

5.3.1 Findings of the Storage Stability Test

The storage-stability results (figure 14) show that adding (NA) and (NS) increased softening-point separation (ΔSP), indicating reduced thermal stability compared with the neat binder (0.5°C). For NA, ΔSP rose from about 0.8°C at 2% to 1.1°C at 4% and 1.6°C at 6%, reflecting a clear decline in stability with dosage. NS showed lower separation, increasing from roughly 0.3°C at 2% to 0.8°C at both 4% and 6%, suggesting better stability than NA at higher contents. Although both nanomaterials exhibit some segregation, all ΔSP values remain within an acceptable range.

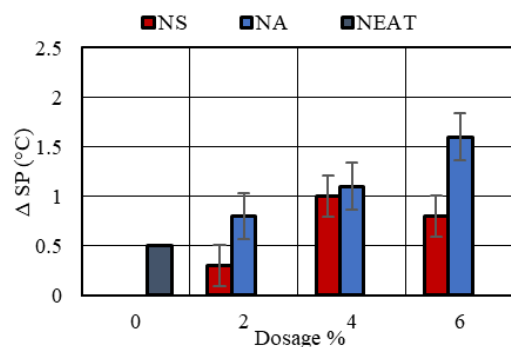


Figure 14. Variation in Asphalt Binder Softening Point (ΔSP) with Different Nanomaterial Dosages.

5.3.2 Microstructure Analysis of Nano-Modified Asphalt Binder

The Scanning Electron Microscopy (SEM) evaluation (Figure 15) demonstrated clear variations in surface morphology between the neat asphalt and the binders modified with nano-silica (NS) and nano-alumina (NA) at concentrations of 2%, 4%, and 6%. The neat asphalt displayed a typically smooth, amorphous, and mildly undulating surface. Incorporation of NS produced a gradual increase in surface roughness and heterogeneity with rising dosage, with the 6% NS sample exhibiting pronounced textural irregularities, reflecting reduced uniformity in particle distribution. In contrast, the NA-modified binders showed more uniform dispersion at lower dosages (2% and 4%). At 6% NA, the surface appeared relatively smooth but characterized by distinct, deeper wrinkle-like features, which may indicate the development of an internal nanoscale reinforcement network, suggesting enhanced compatibility and potentially more favorable

implications for the structural integrity and rheological behavior of the asphalt binder.

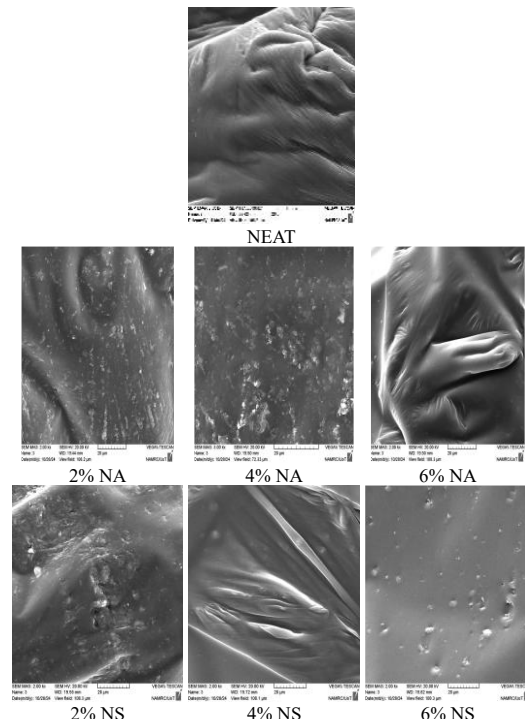


Figure 15. SEM of NEAT and nano-modified asphalt binder.

5.4.1 IDEAL CT Test Results

As presented in figure 16-18, incorporation of (NA) and (NS) induced notable variations in fatigue performance of asphalt binder, which was quantitatively assessed using the CT-Index, Flexibility Index (FI), and Crack Resistance Index (CRI). For NA modified binder, CT-Index increased markedly from 35 in the NEAT binder to 65, 78, and 84 for 2%, 4%, and 6%, respectively, indicating improved resistance to fatigue initiation. FI values exhibited a peak (21.77) at 2%, followed by a slight decline at higher concentrations. This result may imply that moderate NA dosages enhance binder flexibility, whereas excessive addition may compromise ductility. Similarly, CRI reached its maximum at 4% (604.81). Reducing the sensitivity of asphalt mixtures to temperature and stress is an effective approach to prolong their fatigue life, and the application of NA achieves this purpose [58, 59]. In contrast, NS modified binders displayed a distinct trend. The CT-Index attained its highest value at 2% (105), substantially exceeding those of NA modified and NEAT binders, superior initial fatigue resistance at low NS content was observed. However, further increases in NS concentration to

4% and 6% resulted in reduced CT-Index values (59 and 53, respectively), this shows the potential detrimental effects of excessive NS on fatigue performance. When viewing figure 17, FI parameter was decreased progressively with increasing NS content, from 21.85 at 2% to 13.64 at 6%. CRI followed a similar pattern, peaking at 4% (615.53) before declining slightly at NS-6%, suggesting the existence of an optimal NS concentration for crack resistance enhancement.

After the viewing the results, it verified that the incorporation of nanomaterials into asphalt significantly enhances its mechanical performance and durability [60]. Nanoparticles improve the viscoelastic properties of bitumen, increase tensile strain capacity, and delay micro-crack formation, thereby extending fatigue life compared to conventional binder [61,62]. Specifically, NS reduces micro-crack growth and resists creep-induced damage, resulting in higher fatigue life. Similar to NS, the addition of NA also improves fatigue performance and may enhance cohesion and adhesion between the modified bitumen and aggregates, minimizes relative aggregate displacement, and slows down crack initiation and propagation [16]. NA also reduces tensile strain and significantly prolongs the fatigue life of asphalt mixtures. Experimental results show that fatigue life and cumulative dissipated energy (CDE) increase with NS content across different strain levels, reflecting improved energy absorption and cracking resistance [63].

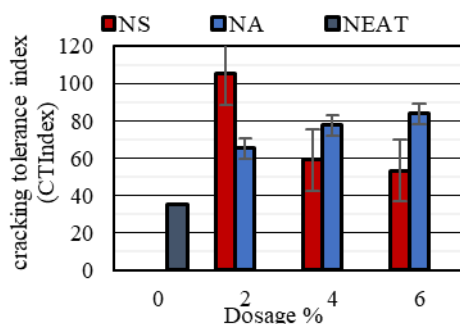


Figure 16. Cracking tolerance of modified asphalt mixture.

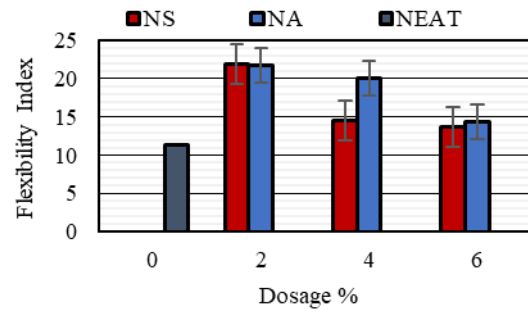


Figure 17. Flexibility Index of modified asphalt mixture.

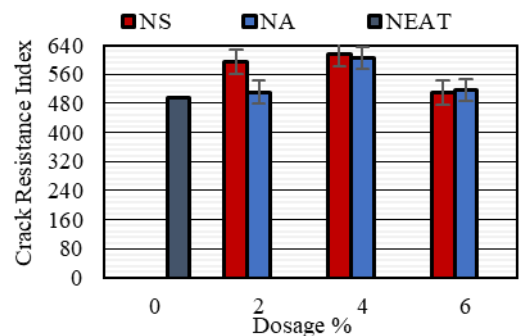


Figure 18. Crack Resistance Index (modified asphalt mixtures).

6. Conclusions

Within the limitations of materials and testing program used in this work, the following principal conclusions are made based on the findings of the investigations:

1. Both of the implemented nanomaterials, NS as well as NA. the physical, rheological and the resistance to fatigue cracking for the asphalt binder and hence asphalt mixtures are substantially improved. The improvement magnitude is mainly dependent on nanomaterials dosage.
2. Based on the physical tests, NA showed the most significant stiffening effect, reflected in a 50% reduction in penetration at 6%, while NS exhibited a pronounced increase in softening point at the same dosage. Rotational viscosity increased consistently for both modifiers, with NS particularly at 6% exhibiting the highest viscosity rise due to its superior surface area and stronger interaction with the binder matrix.

3. The surface roughness of the modified binder as evaluated based on the SEM microstructural analysis showed that NS, specifically at higher dosages is more heterogeneous than those muddled with NA. the latter promoted relatively uniform dispersion and the formation of a nanoscale reinforcement network at higher contents
4. At 4 and 6% dosages, NA improved fatigue resistance. In the other hand, NS performed optimally at 2% and 4%, with performance deterioration observed at 6%. The LAS results support these trends
5. Based on the asphalt concrete mixture performance against fatigue mode of distress, NA showed progressive improvements in CT-Index, FI, and CRI, with CT-Index maximizing at 6%, FI at 2%, and CRI at 4%. NS, conversely, exhibited exceptional fatigue tolerance at low dosage (CT-Index = 105 at 2%), while higher contents (4–6%) reduced flexibility and post-peak ductility, though CRI peaked at 4%, which indicates a narrow optimum window for effective performance.
6. The main findings which can be abstracted from the obtained results revealed that the optimal practical dosage for NS is approximately (2–4%), with 2% being the most effective for balanced fatigue and mechanical performance. Whereas for NA, the optimal dosage range lies between (4–6%), with 6% offering the most comprehensive improvement across binder- and mixture-level.

During this study, the performance was evaluated based on fatigue cracking. Other types of distresses which associated with the high environmental temperature, permanent deformation (rutting) as well as poor water drainage (moisture damage) should be further investigated to prove the overall performance of modified binder using the NS and NA. Also, the synergic use of these two nanomaterials could be further implemented. Also, assessing the economic feasibility, workability implications, and compatibility of these nanomaterials with different binder grades and aggregate types will

support broader implementation in pavement engineering practice.

Conflict of interest

The authors declare no conflicts of interest concerning this research.

Funding

No funding was received for conducting this study.

Author Contribution

A.H. Al Bayati: Supervision, Validation, Methodology, Selection of discussion sections, Writing – review & editing.

A.M. Al Hamdou and Yu Wang: Writing – original draft, Literature collection, Data organization, Writing – review & editing.

AI Declaration Statement

The authors confirm that the manuscript has been written without the assistance of generative AI or AI-based writing tools.

References

- [1] B. Sengoz and A. Topal, “Use of asphalt roofing shingle waste in HMA,” *Constr. Build. Mater.*, vol. 19, no. 5, pp. 337–346, 2005.
<https://doi.org/10.1016/j.conbuildmat.2004.08.005>
- [2] D. Cheng, D. Little, R. Lytton, and J. Holste, “Surface energy measurement of asphalt and its application to predicting fatigue and healing in asphalt mixtures,” *Transp. Res. Rec.*, vol. 1810, pp. 44–53, 2002.
<https://doi.org/10.3141/1810-06>
- [3] R. S. Lakes, *Viscoelastic Materials*. Cambridge, U.K.: Cambridge Univ. Press, 2009.
- [4] C. Hintz, “Understanding mechanisms leading to asphalt binder fatigue,” Ph.D. dissertation, Univ. Wisconsin–Madison, Madison, WI, USA, 2012.
- [5] H. Wen, “Fatigue performance evaluation of WesTrack asphalt mixtures based on viscoelastic analysis of indirect tensile test,” Ph.D. dissertation, North Carolina State Univ., Raleigh, NC, USA, 2001.

- [6] A. F. Mirhosseini et al., "Evaluating fatigue behavior of asphalt binders and mixes containing date seed ash," *J. Civ. Eng. Manag.*, vol. 23, no. 8, pp. 1164–1175, 2017. <https://doi.org/10.3846/13923730.2017.1396560>
- [7] F. Xiao, S. Amirkhanian, and C. H. Juang, "Prediction of fatigue life of rubberized asphalt concrete mixtures containing reclaimed asphalt pavement using artificial neural networks," *J. Mater. Civ. Eng.*, vol. 21, no. 6, pp. 253–261, 2009. [https://doi.org/10.1061/\(ASCE\)0899-1561\(2009\)21:6\(253\)](https://doi.org/10.1061/(ASCE)0899-1561(2009)21:6(253))
- [8] E. Santagata et al., "Correlating creep properties of bituminous binders with anti-rutting performance of corresponding mixtures," *Int. J. Pavement Res. Technol.*, vol. 10, no. 1, pp. 38–44, 2017. <https://doi.org/10.1016/j.ijprt.2016.11.008>
- [9] N. Saboo and P. Kumar, "Performance characterization of polymer modified asphalt binders and mixes," *Adv. Civ. Eng.*, vol. 2016, Art. no. 5938270, 2016. <https://doi.org/10.1155/2016/5938270>
- [10] F. Safaei, C. Castorena, and Y. R. Kim, "Linking asphalt binder fatigue to asphalt mixture fatigue performance using viscoelastic continuum damage modeling," *Mech. Time-Depend. Mater.*, vol. 20, pp. 299–323, 2016. <https://doi.org/10.1007/s11043-016-9304-1>
- [11] C. Fang et al., "Nanomaterials applied in asphalt modification: A review," *J. Mater. Sci. Technol.*, vol. 29, no. 7, pp. 589–594, 2013. <https://doi.org/10.1016/j.jmst.2013.04.008>
- [12] M. Saltan, S. Terzi, and S. Karahancer, "Examination of hot mix asphalt and binder performance modified with nano silica," *Constr. Build. Mater.*, vol. 156, pp. 976–984, 2017. <https://doi.org/10.1016/j.conbuildmat.2017.09.069>
- [13] F. Leiva-Villacorta and A. Vargas-Nordbeck, "Optimum content of nano-silica to ensure proper performance of an asphalt binder," *Road Mater. Pavement Des.*, vol. 20, no. 2, pp. 414–425, 2017. <https://doi.org/10.1080/14680629.2017.1385510>
- [14] H. Nazari, K. Naderi, and F. M. Nejad, "Improving aging resistance and fatigue performance of asphalt binders using inorganic nanoparticles," *Constr. Build. Mater.*, vol. 170, pp. 591–602, 2018. <https://doi.org/10.1016/j.conbuildmat.2018.03.107>
- [15] G. Shafabakhsh, M. Rajabi, and A. Sahaf, "The fatigue behavior of SBS/nanosilica composite modified asphalt binder and mixture," *Constr. Build. Mater.*, vol. 229, Art. no. 116796, 2019. <https://doi.org/10.1016/j.conbuildmat.2019.116796>
- [16] A. Lotfi-Eghlim and M. S. Karimi, "Fatigue behavior of hot mix asphalt modified with nano Al₂O₃—An experimental study," *Adv. Sci. Technol. Res. J.*, vol. 10, no. 31, pp. 58–63, 2016. <https://doi.org/10.12913/22998624/64011>
- [17] S. Karahancer, "Effect of aluminum oxide nanoparticle on modified bitumen and hot mix asphalt," *Pet. Sci. Technol.*, vol. 38, no. 13, pp. 773–784, 2020. <https://doi.org/10.1080/10916466.2020.1783292>
- [18] F. S. Bhat and M. S. Mir, "Investigating the effects of nano Al₂O₃ on high and intermediate temperature performance properties of asphalt binder," *Road Mater. Pavement Des.*, vol. 22, no. 11, pp. 2604–2625, 2020. <https://doi.org/10.1080/14680629.2020.1778509>
- [19] Y. Mamuye, N.-D. Do, and M.-C. Liao, "Nano-Al₂O₃ composite on intermediate and high temperature properties of neat and modified asphalt binders," *SSRN*, 2022. <https://doi.org/10.2139/ssrn.4017442>
- [20] AASHTO M 320, Standard Specification for Performance-Graded Asphalt Binder. Washington, DC, USA: AASHTO, 2013.
- [21] AASHTO T 49, Standard Test Method for Penetration of Bituminous Materials. Washington, DC, USA: AASHTO, 2020.

- [22] AASHTO T 51, Standard Test Method for Ductility of Asphalt Materials. Washington, DC, USA: AASHTO, 2020.
- [23] AASHTO T 53, Standard Test Method for Softening Point of Bitumen (Ring-and-Ball Apparatus). Washington, DC, USA: AASHTO, 2020.
- [24] M. Enieb and A. Diab, "Characteristics of asphalt binder and mixture containing nanosilica," *Int. J. Pavement Res. Technol.*, vol. 10, no. 2, pp. 148–157, 2016. <https://doi.org/10.1016/j.ijprt.2016.11.009>
- [25] G. H. Hamed and N. Esmaeili, "Investigating the effects of nano-materials on moisture susceptibility of asphalt mixtures containing glass cullets," *AUT J. Civ. Eng.*, vol. 3, no. 1, pp. 107–118, 2018. <https://doi.org/10.22060/ajce.2018.14665.5492>
- [26] ASTM D3515-01, Standard Specification for Hot-Mixed, Hot-Laid Bituminous Paving Mixtures. West Conshohocken, PA, USA: ASTM Int., 2001.
- [27] A. H. Albayati et al., "Experimental study to investigate performance-related properties of modified asphalt concrete using nanomaterials Al_2O_3 , SiO_2 , and TiO_2 ," *Materials*, vol. 17, no. 17, Art. no. 4279, 2024. <https://doi.org/10.3390/ma17174279>
- [28] AASHTO T 315-12, Standard Method for Determining Rheological Properties of Asphalt Binder Using Dynamic Shear Rheometer (DSR). Washington, DC, USA: American Association of State Highway and Transportation Officials (AASHTO), 2012.
- [29] AASHTO T 391-20, Standard Method for Determining Asphalt Binder Fatigue Properties Using Linear Amplitude Sweep (LAS) Test. Washington, DC, USA: AASHTO, 2020.
- [30] AASHTO T 240-13, Standard Method for Effect of Heat and Air on Asphalt Binder Using Rolling Thin-Film Oven Test (RTFOT). Washington, DC, USA: AASHTO, 2013.
- [31] AASHTO R 28-12, Standard Practice for Accelerated Aging of Asphalt Binder Using a Pressurized Aging Vessel (PAV). Washington, DC, USA: AASHTO, 2012.
- [32] F. Zhang, J. Yu, and J. Han, "Effects of thermal oxidative ageing on modified asphalts," *Constr. Build. Mater.*, vol. 25, no. 1, pp. 129–137, 2011. <https://doi.org/10.1016/j.conbuildmat.2010.06.048>